

# Monte Carlo method for simulations of adsorbed atom diffusion on a surface

Y.H. Liu <sup>\*</sup>, E. Neyts, A. Bogaerts

*Department of Chemistry, University of Antwerp, Universiteitsplein 1, B-2610 Antwerp, Belgium*

Received 26 July 2005; received in revised form 20 December 2005; accepted 22 January 2006

Available online 28 February 2006

## Abstract

We present a simulation method for describing the diffusion processes of adsorbed atoms on a covalently bound surface. The method takes advantage of the benefit of the Monte Carlo technique for extending the time scale in simulations, and it is independent of the lattice type of the surface. It is particularly useful in the study of the diffusion processes on a surface with structural and/or chemical inhomogeneity. As a simple illustration of the method, we apply it to study hydrogen diffusion on a relaxed regular diamond {111} surface and an irregular diamond {111}-like surface. Four and five local minima for adsorption of a hydrogen atom are found on the regular diamond {111} surface and the irregular surface, respectively. The activation energies, the vibrational frequencies and the total escape rates of the hydrogen atom at each minimum are determined. The mean square displacement and diffusion constant of the hydrogen atom on the surfaces are also calculated. The results indicate that the Monte Carlo method is effective to investigate the diffusion processes of atoms on an arbitrary surface.

© 2006 Elsevier B.V. All rights reserved.

*Keywords:* Monte Carlo simulation; Diffusion; Diamond-like carbon

## 1. Introduction

There is currently considerable interest in the dynamics of atoms and molecules adsorbed on surfaces, due to the key role that surfaces play in a variety of important processes, and because of advances in experimental methods for characterizing surface events [1,2]. The current theoretical understanding of the dynamics of particles on a surface comes largely from computer “experiments,” in which adsorbed atoms or overlayers are evolved dynamically, allowing observation of the physical processes of interest. The molecular-dynamics (MD) [3] simulation method is an extremely powerful tool to study microscopic motion based on the Newtonian dynamics of atoms interacting through a model potential. The equations of motion are solved using a mesh of discrete time steps. The time step of the MD simulations must be short compared with the phonon frequencies, usually a fraction of a femtosecond. Hence, the total simulation time, which is of the order of  $10^7$  to  $10^9$  steps depending on the model potential, is limited to the microsecond region. Non-accelerated MD simulations can be used to simulate atomic processes occurring on a time scale of microseconds at

most. For a variety of physical situations, however, this time scale is far too short to study the true dynamics of a system, in particular for diffusive processes, such as atom diffusion on surfaces, certain formation processes during growth, and defect migration in bulk material [4–6].

An extension of standard MD schemes by Voter [7] focuses on the simulation of such processes. By adding an artificial boosting potential to the true local energy landscape of the atoms, the energy barriers to configurations which are normally not accessible by ordinary MD can be overcome. Thus, the atoms are forced to do movements which are related to barrier heights incompatible with normal thermal activation energies, yielding an extended time scale.

Another class of methods that has been proposed to relax a system over a large period of time is based on the knowledge of the local energy barriers [8,9]. This scheme, which is known as the activation-relaxation technique (ART), has been used in identifying relevant local relaxation processes in amorphous silicon at low temperatures [10]. However, this method also suffers from the fairly general problem whether all saddle points relevant for the evolution of the system can be found.

If the dynamics of a system can be described as a sequence of rather independent infrequent events, long time scales can be modeled using transition-state theory (TST). Since its

<sup>\*</sup> Corresponding author.

E-mail address: [yanhong.liu@ua.ac.be](mailto:yanhong.liu@ua.ac.be) (Y.H. Liu).

development in the thirties, TST has been applied to a wide range of phenomena [11,12]. Dawnkaski et al. used a TST based time dependent Monte Carlo method to simulate the H reactions on the diamond  $\{001\}(2 \times 1)$  surface under chemical vapor deposition (CVD) conditions [13]. Voter developed a TST based kinetic Monte Carlo (KMC) method for describing the dynamics of such infrequent events in a regular lattice and applied it to the study of rhodium clusters on Rh(100) [4]. Srivastava and Garrison performed TST based lattice gas (LG) simulations to investigate the Si adatom self-diffusion on the fully relaxed Si  $\{100\}(2 \times 1)$  surface [14]. In this paper, we present a TST based Monte Carlo method which is more general and can be used to investigate the diffusion processes on a surface with or without a regular lattice. This Monte Carlo algorithm in essence followed that of Gillespie [15]. Netto et al. have adapted this algorithm to investigate the surface processes, such as growth, etching and atom migration on surfaces during a CVD diamond deposition process [16–19]. In Netto and Frenklach paper [16], the particle escape rates are taken from literature or estimated from the corresponding mechanisms. In our paper, the atom escape rates will be calculated after every jump event completed, which makes this Monte Carlo method more general to be used in different applications.

In Section 2 we describe our method in detail. As an example we discuss in Section 3 the diffusion of hydrogen adatoms on a diamond  $\{111\}$  surface and an irregular diamond  $\{111\}$ -like surface. This is an important process during the CVD frequently used to deposit diamond and other thin films [19,20]. A conclusion is given in Section 4.

## 2. Simulation method

The fundamental assumption in TST is that there exists a dividing surface in phase space with two properties: (1) it separates reactants from products and (2) any trajectory crossing this surface will not recross it. The related rate constants which describe the equilibrium flux of particles through the dividing surface can be approximated to a good extent by simple transition state theory (STST) [6]:

$$k^{\text{STST}} = \sum_{i=1,n} v_i \exp[-(E_{\text{saddle}} - E_{\text{min}})/k_{\text{B}}T], \quad (1)$$

where  $n$  is the number of possible diffusion directions of the adatom,  $v_i$  is the harmonic frequency, and  $E_{\text{saddle}}$  and  $E_{\text{min}}$  are the energies at the transition state (i.e. saddle point) between two binding sites and at the minimum, respectively;  $T$  is the temperature and  $k_{\text{B}}$  is the Boltzmann's constant. The second basic TST assumption in practice is violated to a certain extent, since each crossing of the dividing surface does not necessarily correspond to a reactive event. Thus Eq. (1) gives an upper bound to the true rate constant. However, some MD studies show that the STST rate constants give a reasonable approximation to the exact TST rate constants, and also to the dynamically exact rate constants [21].

Provided there exists a systematic way of finding all the minima and saddle points of the energy landscape in the

immediate neighborhood of an adatom one would be able to evolve the system in accord with the STST expression for the rate constant. We have implemented this idea into a Monte Carlo type algorithm in order to study the adatom's diffusion process on a surface with or without a regular lattice. The main procedure of the Monte Carlo method is described as follows:

### 2.1. Choice of the diffusing atoms

In general, all atoms in a given model structure may be involved in the jumps (diffusive events) over energy barriers in their neighborhood. Here, the number of atoms that are explicitly considered is restricted in order to study only such processes that are associated with the surface. In this paper, the atoms which are on the surface and not covered by other atoms are considered to be possible candidates for diffusion. In the following these atoms are called the movers. The number of movers is denoted by  $N_{\text{diff}}$ .

### 2.2. Search for the saddle points and minima around every mover

To avoid extensive calculations, the corresponding saddle points and minima are searched in a small volume around every mover. The volume should also be large enough to ensure that the relevant saddle points and minima are included. The total number of grid points in the volume determines the success rate with which one will be able to find all the local saddle points and minima. Hence, the grid should be sufficiently small.

We use the three-dimensional Newton–Raphson root finding method to search for the saddle points and minima around the mover. If the search converges to an extreme point, then we use the Hessian matrix, which is a  $(3 \times 3)$  matrix of second derivatives of energy for motion of the mover, to determine whether the extreme point is a minimum or saddle point. At each extreme point, we calculate and diagonalize the  $(3 \times 3)$  matrix, and obtain the three eigenvalues and eigenvectors of the matrix. If the matrix has exactly one negative eigenvalue, this point is a saddle point. The negative eigenvalue is in the direction over the saddle point, which will be used to determine along which direction the mover may jump. If the matrix has three positive eigenvalues, then this point is a minimum. At these minima and saddle points, the energies  $E_{\text{saddle}}$  and  $E_{\text{min}}$  are calculated. At the same time, the mover's vibrational frequencies  $\nu_{1\text{m}}$ ,  $\nu_{2\text{m}}$ ,  $\nu_{3\text{m}}$ ,  $\nu_{1\text{s}}$  and  $\nu_{2\text{s}}$  are also obtained from  $\nu_j = (1/2\pi)(b_j/M)^{1/2}$ , where  $b_j$  is the eigenvalue of the  $(3 \times 3)$  matrix, and  $M$  is the atom mass, and  $\nu_{1\text{m}}$ ,  $\nu_{2\text{m}}$ , and  $\nu_{3\text{m}}$  are the vibrational frequencies at the minimum, and  $\nu_{1\text{s}}$  and  $\nu_{2\text{s}}$  are the two non-imaginary vibrational frequencies at the saddle point. Finally, the pre-exponential factor  $v_i$  in Eq. (1) is calculated from

$$v_i = \frac{\nu_{1\text{m}}\nu_{2\text{m}}\nu_{3\text{m}}}{\nu_{1\text{s}}\nu_{2\text{s}}}. \quad (2)$$

After all the saddle points and minima around the mover are found, we use the eigenvectors corresponding to the negative

eigenvalues of the Hessian matrix at the saddle points to determine in which direction the mover may diffuse. As we mentioned before, these eigenvectors are in the directions over the saddle points. The mover must overcome this saddle point properly, i.e. the line linking the initial minimum where the mover is localized and the saddle point should be in the direction that the eigenvector points to. Following this scheme for every mover, all the possible diffusion directions of every mover can be determined.

### 2.3. Choice of a diffusion event

After determination of the possible diffusion directions for every mover, the escape rate  $k_i^{\text{STST}}$  for the mover  $i$  can be calculated by using Eq. (1). The escape rates of the  $N_{\text{diff}}$  movers define a set of local escape rates of the movers from their harmonic basins (i.e. local minima). This set of escape rates can be regarded as a distribution function, from which the specific mover can be determined, which will actually carry out the jump. This is done by drawing a probability, given by  $P_i = k_i^{\text{STST}} / k_{\text{total}}$ , where  $k_{\text{total}} = \sum_{i=1, N_{\text{diff}}} k_i^{\text{STST}}$  is the total escape rates of  $N_{\text{diff}}$  movers. We then use a random number  $R \in (0, 1)$  to determine which mover will jump at this time.

After the effective mover  $i$  is chosen, the diffusion direction  $j$  of mover  $i$  is determined by another random number and probability given by  $P_j = k_{ij} / k_i^{\text{STST}}$ , where  $k_{ij} = v_j \exp[-(E_{\text{saddle}} - E_{\text{min}}) / k_{\text{B}}T]$  is the escape rate of mover  $i$  in the direction  $j$ .

### 2.4. Completion of the diffusive event

After the event, i.e. the specific mover plus its escape direction have been determined from the probabilities  $P_i$  and  $P_j$ , this mover  $i$  is set to its nearest minimum around it in the diffusion direction  $j$ . The time clock is incremented by  $\Delta t_{\text{hop}} = 1 / k_i^{\text{STST}}$ , where  $k_i^{\text{STST}} = \sum_{j=1, n} k_{ij}$  is the total escape rate of mover  $i$  from its initial minimum, i.e. the sum of the escape rates of mover  $i$  in its  $n$  possible diffusion directions [6]. It should be pointed out that our time increment  $\Delta t_{\text{hop}}$  yields only a lower limit of the time duration while it assumes that any of the diffusion jumps has taken place. A more rigorous way to define the time increment is given by Netto and Frenklach [16] and Battaile et al. [22].

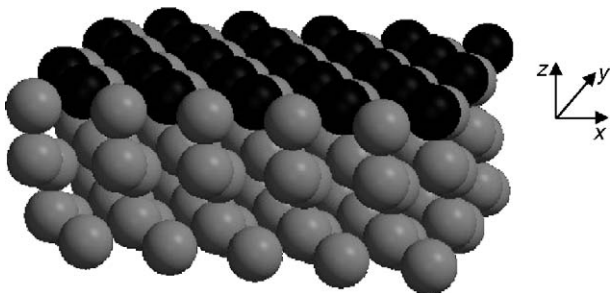


Fig. 1. Three-dimensional picture of the relaxed diamond substrate consisting of a 6-layer thick carbon slab with 25 atoms per layer. The surface atoms are indicated in black and the other atoms are grey.

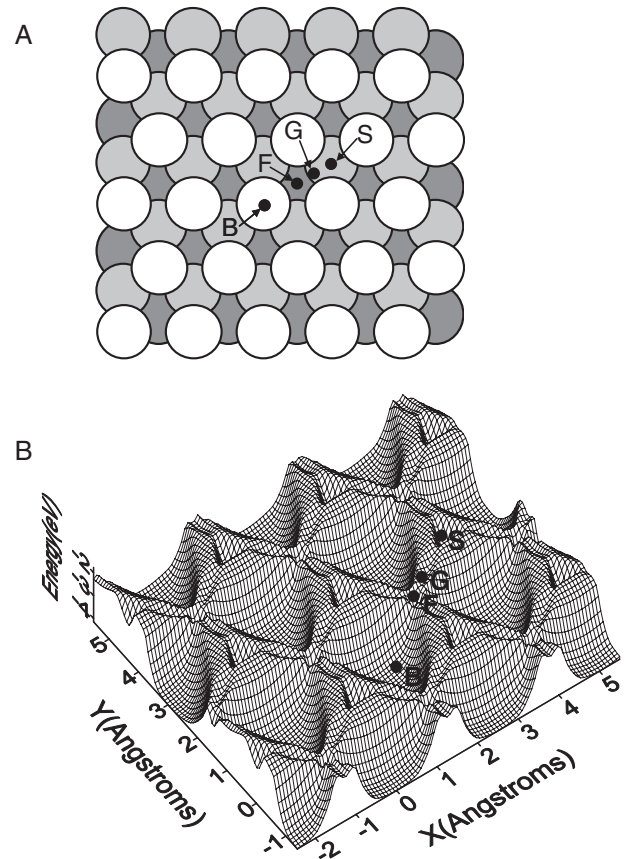


Fig. 2. Schematic picture of the regular diamond {111} surface. (A) The surface with unique binding sites labelled with B, F, G and S. The atoms are indicated as white, light grey and dark grey in the first, second and fourth layer, respectively. The atoms in the third layer are overlapped by the atoms in the second layer. (B) Energy profile for a single H adatom on the surface, the letters B, F, G and S denote the unique binding sites.

### 2.5. Update of the escape rates

Because the local environment of every mover may be changed considerably due to the last diffusion event, the local escape rates of the various movers also need to be updated before defining the next successful jump event. This step is done in the same way as described above in Sections 2.1, 2.2 and 2.3. Note that movers may change their status from being defined as “movers” to “non-movers” or vice versa in the simulations according to the definition of a mover (see Section 2.1).

## 3. Illustration of the simulation results and discussions

### 3.1. Diffusion of a single H adatom on a relaxed diamond {111} surface

To illustrate our Monte Carlo method, we investigate hydrogen diffusion on a relaxed diamond {111} surface. The simulation system consists of a 6 layer thick carbon slab with 25 atoms per layer (see Fig. 1). Periodic boundary conditions are used in the  $\pm x$  and  $\pm y$  directions of the system. The relaxed diamond {111} system is obtained in the following manner. All of the atoms in the system are initially given lattice sites

corresponding to the pure unstrained system. The periodic boundary conditions parallel to the  $\{111\}$  surface plane maintain the horizontal lattice constant to be that of the unstrained substrate; whereas, in the plane perpendicular to the  $\{111\}$  surface the crystal is allowed to relax freely via the forces derived from the Brenner potential [23]. This procedure is done by heating the crystal to 300K for a period of approximately 50ps during which time the atoms move to positions corresponding to a lower energy configuration. The system is then cooled slowly for an additional 50ps to near 0K.

In the following simple illustration, the carbon atoms in the relaxed substrate are assumed fixed, and a single hydrogen adatom (i.e.,  $N_{\text{diff}}=1$ ) is diffusing on the relaxed diamond  $\{111\}$  surface. We consider the diffusion process as a sequence of jumps from one stable site (i.e. minimum) to another on the surface. The Brenner potential is chosen to calculate the atomic interactions and, hence, the energies at the minima and the saddle points. It should be pointed out that although the Brenner potential is not the most accurate potential to calculate the potential energy at surfaces [24], this potential is still very useful for our simulations to calculate the surface energy in a relatively short time [25]. Calculations based on an ab initio potential would yield extremely long calculation time, and the advantage of modeling surface diffusion by using a Monte Carlo method (i.e., to increase the speed of the simulation of atom diffusion) would become lower. In this paper, in view of the fact that our main purpose is to demonstrate the efficiency of the Monte Carlo method to investigate the atom diffusion on a surface, the Brenner potential is adopted. In future studies, for a better description of the surface energy, other more accurate potentials may be adopted [24,26]. The possible impact of the Brenner potential on our simulation results is discussed in the following sections.

### 3.1.1. Surface structure and energy profile for a single H adatom on the relaxed diamond $\{111\}$ surface

Following the procedure outlined above we calculated the energy profile of a single H adatom on the relaxed diamond  $\{111\}$  surface. Fig. 2A shows the relaxed diamond  $\{111\}$  surface with unique binding sites (i.e. minima) labeled as  $B$ ,  $F$ ,  $G$  and  $S$ . Fig. 2B shows the energy profile for a single H adatom on the surface. The four local minima are identified by a letter and the number of nearest neighbor atoms in the surface and subsurface (i. e. second layer) of the substrate, respectively. The  $B(1,3)$  and  $S(3,1)$  sites are the on-top sites over the bulk terminated first layer atom and over the second layer atom, respectively. The hollow  $F(3,3)$  site is over the fourth layer

Table 2

The H adatom diffusion dynamics on the relaxed diamond  $\{111\}$  surface at 1100K

Jump type	Activation energy (eV)	Vibrational frequency ( $\text{s}^{-1}$ )	Total escape rates ( $\text{s}^{-1}$ )
$B \rightarrow F$	1.97	$5.29 \times 10^{12}$	$1.77 \times 10^4$
$B \rightarrow S$	2.37	$6.21 \times 10^{13}$	
$F \rightarrow G$	0.75	$8.39 \times 10^{13}$	$1.23 \times 10^{11}$
$F \rightarrow B$	0.93	$1.40 \times 10^{14}$	
$G \rightarrow S$	0.52	$4.46 \times 10^{13}$	$1.76 \times 10^{13}$
$G \rightarrow F$	0.03	$2.27 \times 10^{13}$	
$S \rightarrow G$	0.82	$2.23 \times 10^{14}$	$5.87 \times 10^{11}$
$S \rightarrow B$	0.91	$2.24 \times 10^{15}$	

atom, and the  $G(2,1)$  site is midway between site  $F(3,3)$  and  $S(3,1)$ . The locations of these four local minima are very similar to the important interstitial sites, i.e., BC-site,  $T$ -site and  $H$ -site, of a single hydrogen atom in diamond [6,27–30]. Indeed, the  $B(1,3)$  site is similar to the BC-site which is the bond-centered site and is the midpoint between two carbon atom sites. The  $F(3,3)$  and  $S(3,1)$  sites are similar to the  $T$ -site which lies equidistant from four carbon sites. The  $G(2,1)$  site is similar to the  $H$ -site which lies midway between two  $T$ -sites. Their geometries and energies are given in Table 1.

### 3.1.2. Energetics and diffusion of a H adatom on the relaxed diamond $\{111\}$ surface

From Table 1, one can see that the global minimum for the surface occurs at site  $B$  ( $E=-4.15\text{eV}$ ). This  $B$  site has a large region of the surface over which the adsorption can occur. The other sites  $F$ ,  $G$  and  $S$  have a higher energy and narrower region onto which the incoming atom can be adsorbed. These features of the energy profiles indicate that adsorption on site  $B$  would be more probable than adsorption on sites  $F$ ,  $G$  and  $S$ . So, the  $B$  site must be more stable, and the residence time of an H adatom at this site is much longer than at other sites.

To determine the escape rates we have also calculated the activation barriers (given in Table 2) between these sites. The corresponding jump frequencies and the escape rates are also calculated and given in Table 2. The activation barriers vary from 0.03 eV ( $G \rightarrow F$ ) to 2.37 eV ( $B \rightarrow S$ ). The calculated vibrational frequencies used as prefactors in Eq. (1) have values ranging from  $5.29 \times 10^{12} \text{ s}^{-1}$  to  $2.24 \times 10^{15} \text{ s}^{-1}$ . The calculated escape rates from the various sites vary from  $1.77 \times 10^4 \text{ s}^{-1}$  to  $1.76 \times 10^{13} \text{ s}^{-1}$  at a temperature of 1100K. Correspondingly, the residence times vary from  $5.66 \times 10^{-5} \text{ s}$  to  $5.68 \times 10^{-14} \text{ s}$ . Naturally the longest residence time is for site  $B$ , the most stable site. Our results also show that the diffusion of hydrogen on the surface does not occur between neighboring  $B$  sites, and only occurs between  $B$  and  $F$ ,  $F$  and  $G$ , or  $G$  and  $S$  sites. These results are consistent with the results of Kaukonen et al. [6]. It should also be pointed out that the escape rates calculated from the Brenner potential might be smaller than those calculated from the molecular anharmonic potentials with switching (MAPS) functions, derived from ab initio calculations [24]. Some studies show that the Brenner potential does not seem to accurately describe the long-range interactions while accurately representing short-range properties of diamond materials [24].

Table 1

Geometries and energies of a H adatom on the relaxed diamond  $\{111\}$  surface

Site	Adatom height <sup>a</sup> (Å)	Energy (eV)
$B(1,3)$	1.08	-4.15
$F(3,3)$	0.00	-3.10
$G(2,1)$	0.57	-2.38
$S(3,1)$	0.93	-2.68

<sup>a</sup> The adatom height is relative to the position of surface atoms on the relaxed diamond  $\{111\}$  surface.

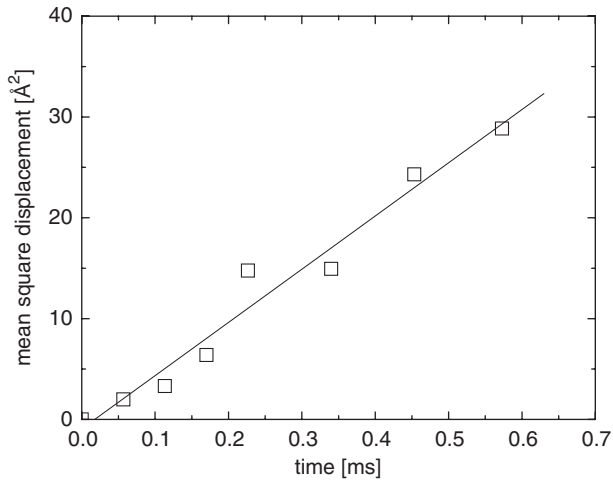


Fig. 3. Calculated mean square displacement of the H adatom on the regular diamond {111} surface as a function of time.

This fact may cause the time increment ( $\Delta t_{\text{hop}} = 1/k_i^{\text{STST}}$ ) in our simulations to become larger, and the atom diffusion constants (calculated below) to become smaller than those calculated from the MAPS potential. However, the comparison between our results and the results of Kaukonen et al. [6] shows that the Brenner potential still can give reasonable results in our simulations.

### 3.1.3. Diffusion constant of the H adatom on the surface

During a long simulation time, thousands of randomly generated jumps can be made and the mean square displacement of the adatom,  $\langle \Delta r^2(t) \rangle$  could be evaluated as a function of the time,  $t$ . The slope of the long time portion of this curve yields the macroscopic diffusion constant,  $D$  [6,31]. In the simulation, the diffusion constant  $D$  can be evaluated by calculating it directly from

$$D = \lim_{t \rightarrow \infty} \left\{ \frac{d}{dt} \left\langle \frac{1}{N_{\text{diff}}} \sum_{i=1}^{N_{\text{diff}}} |\bar{r}_i(t) - \bar{r}_i(0)|^2 \right\rangle \right\} \quad (3)$$

where the average is an ensemble average,  $N_{\text{diff}}$  is the number of diffusing adatoms, and  $r_i(t)$  indicates the position of the  $i$ th adatom at time  $t$ . We have calculated the adatom's mean square displacement as well as the diffusion constant. Fig. 3 shows the time evolution of the mean square displacements of the diffusing H atom for a time period  $\Delta t = 0.6$  ms. A linear dependency is found, in accordance to the Einstein–Smoluchowski theory [31]. According to Eq. (3), we obtain the diffusion constant  $D = 1.32 \times 10^{-12} \text{ cm}^2/\text{s}$ . This value is a little bit higher than the value in Ref. [6] ( $D = 9 \times 10^{-13} \text{ cm}^2/\text{s}$ ). However, in Ref. [6], the H atom is diffusing inside diamond, and it must overcome the restrictions from other atoms localized above it, and hence its diffusion constant is reduced. In our case, there are no atoms situated above the diffusing atom, and the diffusion constant of the H atom is therefore expected to be indeed higher than the value for diffusion inside diamond.

### 3.2. Diffusion of many H adatoms on an irregular diamond {111}-like surface

As mentioned before, this Monte Carlo method can also be applied to cases in which the surfaces are irregular, i.e. multiple crystal layers are simultaneously exposed, e.g., for treating the diffusion of adatoms over a stepped surface, or in modeling amorphous thin film (e.g. diamond-like carbon) growth or surface roughening. Additionally, in experiments, many adatoms on a surface may diffuse simultaneously within a time period. So, we simulate the diffusion process of many H adatoms on an irregular diamond {111}-like surface. The surface is similar to the previous relaxed diamond {111} surface, but in order to make an irregular surface, we remove two atoms from the first layer of the relaxed diamond {111} surface, which is shown in Fig. 4A. The periodic boundary conditions are also used in the  $\pm x$  and  $\pm y$  directions of the system. The layers are assumed fixed during the adatoms diffusion processes. As an illustration, we only choose the number of the diffusing adatoms as  $N_{\text{diff}} = 3$  to limit the complexity of the simulation.

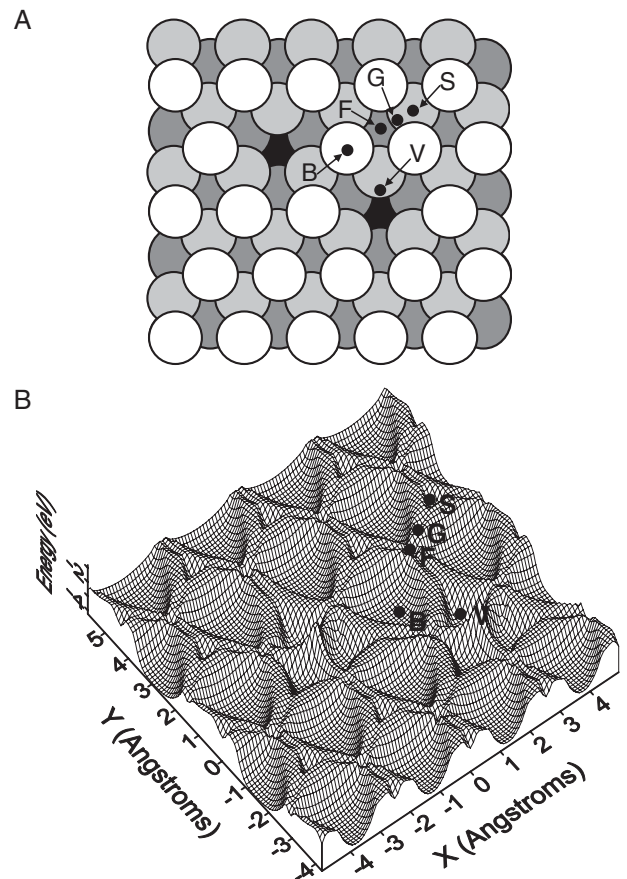


Fig. 4. The irregular diamond {111}-like surface. (A) The surface with unique binding sites labelled with B, F, G, S and V. The atoms are white, light grey, dark grey and black in the first, second, fourth and sixth layer, respectively. The atoms in the third and fifth layer are overlapped by the atoms in the second and fourth layer, respectively. (B) Energy profile for a single H adatom on the surface, the letters B, F, G, S and V denote the unique binding sites.

Table 3

The activation energies, vibrational frequencies and total escape rate of a H adatom from the site  $V$  on the irregular diamond  $\{111\}$ -like surface at 1100K

Jump type	Activation energy (eV)	Vibrational frequency ( $s^{-1}$ )	Total escape rates ( $s^{-1}$ )
$V \rightarrow B$	1.67	$2.06 \times 10^{13}$	$1.90 \times 10^6$
$V \rightarrow F$	1.66	$1.60 \times 10^{13}$	
$V \rightarrow G$	1.63	$4.18 \times 10^{12}$	

### 3.2.1. Surface structure, energy profile and energetics of the H adatoms diffusing on the irregular diamond $\{111\}$ -like surface

Fig. 4A shows the irregular diamond  $\{111\}$ -like surface with unique binding sites (i.e. minima) labeled as  $B$ ,  $F$ ,  $G$ ,  $S$  and  $V$ ; Fig. 4B shows the energy profile for a single H adatom on the surface. A new local minimum  $V(2,1)$  is observed on the surface, beside the other four local minima  $B$ ,  $F$ ,  $G$  and  $S$  discussed in Section 3.1. At the  $V$  site, the adatom height is  $0.05 \text{ \AA}$  relative to the position of the atoms in the first layer, and its potential energy is  $-4.18 \text{ eV}$ , which is very close to the energy of a H adatom at the  $B$  site ( $E = -4.14 \text{ eV}$ ). From Fig. 4A, one can see that the  $B$  and  $V$  sites both have a large region of the surface over which the adsorption can occur. The other sites  $F$ ,  $G$  and  $S$  have a higher energy and narrower region into which incoming atom can be adsorbed. The region for the  $B$  site is still larger than that for the  $V$  site. These features of the energy profiles indicate that adsorption into  $B$  and  $V$  sites would be more probable than adsorption into sites  $F$ ,  $G$  and  $S$ , and the residence time of adatoms at  $B$  and  $V$  sites should be much longer than that at other sites. We have calculated the activation energies, jump frequencies and the total escape rate for a H adatom to escape from site  $V$  to other sites on the surface, and the results are given in Table 3. Note that the escape rates for H adatoms from sites  $B$ ,  $F$ ,  $G$  and  $S$  which are far away from the  $V$  site remain the same as given in Table 2. However, the escape rates from sites  $B$ ,  $F$ ,  $G$  which are near to the site  $V$  are influenced by the removal of the two carbon atoms from the surface, and the total escape rates of a H adatom from the  $B$  and  $F$  sites are increased to  $5.74 \times 10^5 \text{ s}^{-1}$  and  $2.27 \times 10^{12} \text{ s}^{-1}$ , respectively, and the total escape rate from  $G$  site is decreased to  $5.96 \times 10^{12} \text{ s}^{-1}$ . The corresponding residence time of the adatom at these sites  $B$ ,  $F$  and  $G$  are  $1.74 \times 10^{-6} \text{ s}$ ,  $4.41 \times 10^{-13} \text{ s}$  and  $1.68 \times 10^{-13} \text{ s}$ , respectively. The total escape rate of a H adatom from the  $V$  site is  $1.9 \times 10^6 \text{ s}^{-1}$  at a temperature of 1100K. Correspondingly, the residence time of the adatom at site  $V$  is  $5.26 \times 10^{-7} \text{ s}$ . Comparing this value with the residence time of  $5.66 \times 10^{-5} \text{ s}$  and  $1.74 \times 10^{-6} \text{ s}$  of an H adatom at site  $B$  which is far from and near to the site  $V$ , respectively, we can conclude that the site  $B$  is still the most stable site, and site  $V$  is the second stable site on the irregular surface.

### 3.2.2. Diffusion constant of the H adatom on the irregular diamond $\{111\}$ -like surface

We have calculated the adatom's mean square displacement as well as the diffusion constant according to Eq. (3). In Eq. (3), the number of diffusing adatoms is  $N_{\text{diff}}=3$ , i.e. the contributions of the three diffusing adatoms to the mean square displacement and diffusion constant are taken into account. Fig. 5

shows the time evolution of the mean square displacements of the diffusing H adatoms for a time period  $\Delta t=1.6 \text{ ms}$ . A linear dependency is found, and the diffusion constant is then calculated as  $D=1.22 \times 10^{-13} \text{ cm}^2/\text{s}$ . This value is much lower than the diffusion constant ( $D=1.32 \times 10^{-12} \text{ cm}^2/\text{s}$ ) of a H adatom diffusing on the regular diamond  $\{111\}$  surface discussed in Section 3.1. This is due to the irregular surface: some defects are introduced by removing two carbon atoms in the first layer of the substrate, and a relatively stable site  $V$  is produced beside the other stable sites  $B$ ,  $F$ ,  $G$  and  $S$  on the surface. Therefore the diffusing adatoms may stay at the most stable site  $B$  and second stable site  $V$  for a long time, and hence the adatom diffusion constant is greatly reduced.

## 4. Summary

We developed a TST based Monte Carlo method for describing the diffusion process of an adatom on a covalently bonded surface without assuming a regular lattice. With this method the time scale of a simulation is extended such that a much longer simulation time can be achieved compared to ordinary MD. The increase of the time scale depends only on the height of the true energy barriers of the system under consideration and there are no uncertain parameters such as boosting potentials or artificial activation energies needed to evolve the system. In this method, after finishing a jump of an adatom, the local geometries around all the adatoms are reconsidered and their escape rates are updated, such that many-atom jumps can be induced.

We illustrated the method by a simple investigation of hydrogen diffusion on a relaxed regular diamond  $\{111\}$  surface and an irregular diamond  $\{111\}$ -like surface. On the regular diamond  $\{111\}$  surface, four stable sites  $B$ ,  $F$ ,  $G$  and  $S$ , which are very similar to the important interstitial sites, i.e., BC-site, T-site and H-site, of a single hydrogen atom in diamond are observed. The most stable site is the  $B$  site. The diffusion of hydrogen on the surface does not occur between neighboring  $B$  sites, and only occurs between  $B$  and  $F$ ,  $F$  and  $G$ , or  $G$  and  $S$

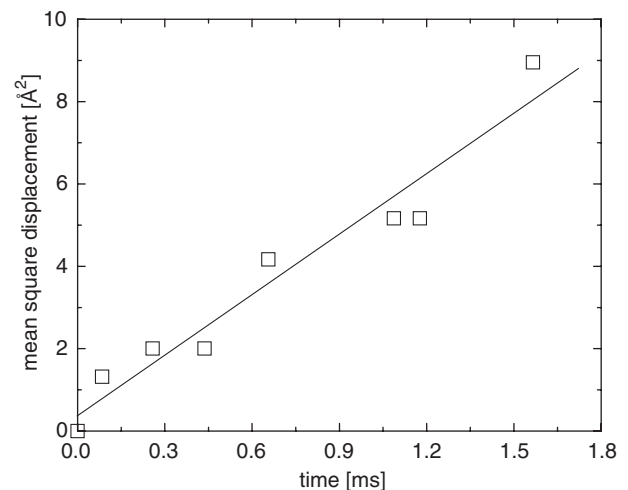


Fig. 5. Calculated mean square displacement of the H adatoms on the irregular diamond  $\{111\}$ -like surface as a function of time.

sites. The mean square displacement and diffusion constant of a H adatom on the regular surface are also calculated. The diffusion constant is a little bit higher than the value of diffusion constant inside diamond. On the irregular diamond {111}-like surface, an additional stable site  $V$  is observed, beside the other four sites  $B$ ,  $F$ ,  $G$  and  $S$ . The  $B$  site is still the most stable site, but the  $V$  site is the second stable site for the H adatom adsorption on the surface. The mean square displacement and diffusion constant of the adatoms on the surface are also calculated. The results show that the adatom diffusion constant is reduced greatly by the defects on the irregular surface. Finally, we would like to emphasize again that although the imprecision of the Brenner potential in calculating the surface energies may cause the obtained atom escape rates and the atom diffusion constants to become smaller than those obtained from the MAPS potential, the comparison between our results and the results of Kaukonen et al. indicates that the Brenner potential still can give relatively reasonable results in our simulations. The illustrations performed in this paper indicate that this TST based Monte Carlo method is effective to investigate the diffusion process of adatoms on regular or irregular surfaces.

### Acknowledgments

Y. H. Liu acknowledges the University of Antwerp (GOA project) for financial support. E. Neyts is indebted to the Institute for the Promotion of Innovation by Science and Technology in Flanders (IWT-Flanders) for financial support. The authors also thank Profs. R. Gijbels, B. J. Thijsse, B. J. Garrison and Dr. Z. Y. Chen for many helpful discussions.

### References

- [1] D. Srivastava, B.J. Garrison, D.W. Brenner, *Phys. Rev. Lett.* 63 (1989) 302.
- [2] J.Y. Tsao, E. Chason, U. Köhler, R. Hamers, *Phys. Rev. B* 40 (1989) 11951.
- [3] E. Neyts, A. Bogaerts, R. Gijbels, J. Benedikt, M.C.M. van de Sanden, *Diamond Relat. Mater.* 13 (2004) 1873.
- [4] A. Voter, *Phys. Rev. B* 34 (1986) 6819.
- [5] J. Krug, F. Hontinfinde, *J. Phys. A* 30 (1997) 7739.
- [6] M. Kaukonen, J. Peräjoki, R.M. Nieminen, *Phys. Rev. B* 61 (2000) 980.
- [7] A. Voter, *J. Chem. Phys.* 106 (1997) 4665.
- [8] G.T. Barkema, N. Mousseau, *Phys. Rev. Lett.* 77 (1996) 4358.
- [9] N. Mousseau, G.T. Barkema, *Phys. Rev., E Stat. Phys. Plasmas Fluids Relat. Interdiscip. Topics* 57 (1998) 2419.
- [10] G.T. Barkema, N. Mousseau, *Phys. Rev. B* 62 (2000) 4985.
- [11] G. Vineyard, *J. Phys. Chem. Solids* 3 (1957) 121.
- [12] M. Gillan, *Phys. Rev. Lett.* 58 (1987) 563.
- [13] E.J. Dawnkaski, D. Srivastava, B.J. Garrison, *J. Chem. Phys.* 102 (1995) 9401.
- [14] D. Srivastava, B.J. Garrison, *J. Chem. Phys.* 95 (1991) 6885.
- [15] D.T. Gillespie, *J. Phys. Chem.* 81 (1977) 2340.
- [16] A. Netto, M. Frenklach, *Diamond Relat. Mater.* 14 (2005) 1630.
- [17] M. Frenklach, *J. Chem. Phys.* 97 (1992) 5794.
- [18] M. Frenklach, *Phys. Rev. B* 45 (1992) 9455.
- [19] M. Frenklach, S. Skokov, *J. Phys. Chem. B* 101 (1997) 3025.
- [20] K. Kobashi, K. Nishimura, Y. Kawate, T. Horiuichi, *Phys. Rev. B* 38 (1988) 4067.
- [21] A. Voter, J. Doll, *J. Chem. Phys.* 82 (1985) 80.
- [22] C.C. Battaile, D.J. Srolovitz, J.E. Butler, *J. Appl. Phys.* 82 (1997) 6293.
- [23] D.W. Brenner, *Phys. Rev. B* 42 (1990) 9458.
- [24] P. de Sainte Claire, K. Song, W.L. Hase, D.W. Brenner, *J. Phys. Chem.* 100 (1996) 1761.
- [25] X.Y. Chang, D.L. Thompson, L.M. Raff, *J. Phys. Chem.* 97 (1993) 10112.
- [26] B.J. Garrison, D. Srivastava, *Annu. Rev. Phys. Chem.* 46 (1995) 373.
- [27] S. Estreicher, A.K. Ray, J.L. Fry, Dennis S. Marynick, *Phys. Rev. B* 34 (1986) 6071.
- [28] C. Chu, S. Estreicher, *Phys. Rev. B* 42 (1990) 9486.
- [29] J.P. Goss, *J. Phys. C* 15 (2003) R551.
- [30] T.L. Estle, S. Estreicher, D.S. Marynick, *Phys. Rev. Lett.* 58 (1987) 1547.
- [31] T. Zambelli, J. Trost, J. Wintterlin, G. Ertl, *Phys. Rev. Lett.* 76 (1996) 795.